9902 *Inorg. Chem.* **2010**, *49*, 9902–9908
DOI: 10.1021/ic1008957

Inorganic Chemistry
Article

One-Pot Conditional Self-Assembly of Multicopper Metallacycles

Kom-Bei Shiu,*,† Shih-An Liu,† and Gene-Hsiang Lee‡

†*Department of Chemistry, National Cheng Kung University, Tainan, Taiwan 701, and*
‡*Instrument Center, National Taiwan University, Taipei, Taiwan 106*

Received May 10, 2010

The self-assembly of supramolecular metallacycles via the coordination-driven directional bonding approach can be modified to produce some unexpected structural variations. The combination of a flexible ligand-capped dinuclear transition-metal acceptor like $[Cu_2(dppm)_2(NCMe)_2]X_2$ (**1**X_2; dppm = $Ph_2PCH_2PPh_2$; X^- = BF_4^-, PF_6^-, or BPh_4^-) with monodentate−bidentate donors like 2-, 3-, and 4-pyridylcarboxylates produced oligomeric compounds $[\{Cu_2(dppm)_2\}(\mu\text{-}(2\text{-}PyCO_2))]_2X_2$ (**2**X_2), $[\{Cu_2(dppm)_2\}(\mu\text{-}(3\text{-}PyCO_2))]_2X_2$ (**3**X_2), and $[\{Cu_2(dppm)_2\}(\mu\text{-}(4\text{-}PyCO_2))]_4X_4$ (**4**X_4), respectively, as the thermodynamically stable products in one-pot reactions. However, the modified self-assembly is still subject to steric hindrance. The reaction of complex **1**$(BF_4)_2$ with 6-Me-3-$PyCO_2H$ did not produce a polygonal dimeric metallacycle but a simple dinuclear complex, $[Cu_2(dppm)_2(6\text{-}Me\text{-}3\text{-}PyCO_2)](BF_4)$ (**5**(BF_4)). The crystal structures of complexes **2**$(PF_6)_2$, **3**$(PF_6)_2$, **4**$(BF_4)_4$, and **5**(BF_4) were determined using X-ray diffraction.

Introduction

Supramolecular metallacycles have recently attracted a lot of attention due to their potential application in areas as diverse as selective guest encapsulation for chemical sensing,[1] reaction catalysis,[2] photoinitiated energy transfer,[3] and intermolecular electron transfer.[4] These metallacycles can be rationally designed and synthesized via the coordination-driven directional bonding approach that combines rigid ligand-capped transition-metal acceptors and multibranched monodentate or multibranched chelate donors with relative ease in a one-pot reaction.[5] A series of reports contributed by Hor et al.[6] demonstrated that the approach is even applicable in cases with mixed-type donors such as pyridylcarboxylate, which contains both the monodentate (i.e., the pyridyl nitrogen atom) and the bidentate (i.e., the carboxyl group) moieties. The combination of rigid ligand-capped transition-metal complexes such as $[Pt(PPh_3)_2(MeCN)_2](OTf)_2$ (OTf^- = $CF_3SO_3^-$) with pyridylcarboxylate ligands afforded predictive compounds based on the shape of the ligands. For ligands, the turning angles of 60°, 120°, and 180° between the pyridyl donor and the carboxylate donor sites for 2-, 3-, and 4-pyridylcarboxylates, respectively, affect the formation of either mononuclear complex or polygonal products, including $[Pt(2\text{-}PyCO_2)(PPh_3)_2](OTf)$, $[Pt(3\text{-}PyCO_2)((PPh_3)_2)]_3(OTf)_3$, and $[Pt(4\text{-}PyCO_2)((PPh_3)_2)]_4(OTf)_4$.[6d] However, the present study shows that the employment of a flexible ligand-capped transition-metal acceptor such as $[Cu_2(dppm)_2(NCMe)_2]^{2+}$ (dppm = $Ph_2PCH_2PPh_2$)[7] can convert various pyridylcarboxylate donors into all polygonal oligomeric compounds.

The cation, $[Cu_2(dppm)_2(NCMe)_2]^{2+}$, contains two copper atoms doubly bridged by two dppm ligands, probably at a *d*(Cu···Cu) of around 3.4 Å with no appreciable cuprophilic interaction.[8] Since this cation has good bonding

*To whom the correspondence should be addressed. E-mail: kbshiu@mail.ncku.edu.tw.

(1) (a) Mines, G. A.; Tzeng, B.-C.; Stevenson, K. J.; Li, J.; Hupp, J. T. *Angew. Chem., Int. Ed.* **2002**, *41*, 154. (b) Kumazawa, K.; Biradha, K.; Kusukawa, T.; Okano, T.; Fujita, M. *Angew. Chem., Int. Ed.* **2003**, *42*, 3909. (c) Kumar, A.; Sun, S.-S.; Lees, A. J. *Coord. Chem. Rev.* **2008**, *252*, 922.

(2) (a) Ito, H.; Kusukawa, T.; Fujita, M. *Chem. Lett.* **2000**, 598. (b) Merlau, M. L.; Mejia, S. D. P.; Nguyen, S. T.; Hupp, J. T. *Angew. Chem., Int. Ed.* **2001**, *40*, 4239. (c) Fiedler, D.; Leung, D. H.; Bergman, R. G.; Raymond, K. N. *Acc. Chem. Res.* **2005**, *38*, 349.

(3) Splan, K. E.; Massari, A. M.; Morris, G. A.; Sun, S.-S.; Reina, E.; Nguyen, S. T.; Hupp, J. T. *Eur. J. Inorg. Chem.* **2003**, 2348.

(4) (a) Lau, V. C.; Berben, L. A.; Long, J. R. *J. Am. Chem. Soc.* **2002**, *124*, 9042. (b) Dinolfo, P. H.; Williams, M. E.; Stern, C. L.; Hupp, J. T. *J. Am. Chem. Soc.* **2004**, *126*, 12989. (c) Dinolfo, P. H.; Hupp, J. T. *J. Am. Chem. Soc.* **2004**, *126*, 16814.

(5) (a) Olenyuk, B.; Stang, P. J. *Acc. Chem. Res.* **1997**, *30*, 502. (b) Leninger, S.; Olenyuk, B.; Stang, P. *J. Chem. Rev.* **2000**, *100*, 853. (c) Swiegers, G. F.; Malefetse, T. *J. Chem. Rev.* **2000**, *100*, 3483. (d) Fujita, M.; Umemoto, K.; Yoshizawa, M.; Fujita, N.; Kusukawa, T.; Biradha, K. *Chem. Commun.* **2001**, 509. (e) Holliday, B. J.; Mirkin, C. A. *Angew. Chem., Int. Ed.* **2001**, *40*, 2022. (f) Cotton, F. A.; Lin, C.; Murillo, C. A. *Acc. Chem. Res.* **2001**, *34*, 759. (g) Seidel, S. R.; Stang, P. J. *Acc. Chem. Res.* **2002**, *35*, 972. (h) Ruben, M.; Rojo, J.; Romero-Salgurero, F. J.; Uppadine, L. H.; Lehn, J.-M. *Angew. Chem., Int. Ed.* **2004**, *43*, 3644. (i) Steel, P. J. *Acc. Chem. Res.* **2005**, *38*, 243. (j) Fujita, M.; Tominaga, M.; Hori, A.; Therrien, B. *Acc. Chem. Res.* **2005**, *38*, 369. (k) Gianneschi, N. C.; Masar, M. S.; Mirkin, C. A. *Acc. Chem. Res.* **2005**, *38*, 825. (l) Stang, P. J. *J. Org. Chem.* **2009**, *74*, 2.

(6) (a) Teo, P.; Koh, L. L.; Hor, T. S. A. *Inorg. Chem.* **2003**, *42*, 7290. (b) Teo, P.; Foo, D. M. J.; Koh, L. L.; Hor, T. S. A. *Dalton Trans.* **2004**, *20*, 3389. (c) Teo, P.; Koh, L. L.; Hor, T. S. A. *Inorg. Chim. Acta,* **2006**, *359*, 3435. (d) Teo, P.; Koh, L. L.; Hor, T. S. A. *Chem. Commun.* **2007**, 2225. (e) Teo, P.; Koh, L. L.; Hor, T. S. A. *Inorg. Chem.* **2008**, *47*, 6464. (f) Teo, P.; Koh, L. L.; Hor, T. S. A. *Inorg. Chem.* **2008**, *47*, 9561.

(7) Diez, J.; Gamasa, M. P.; Gimeno, J.; Tiripicchio, A.; Camellini, M. T. *J. Chem. Soc., Dalton Trans.* **1987**, 1275.

Published on Web 10/07/2010

Scheme 1

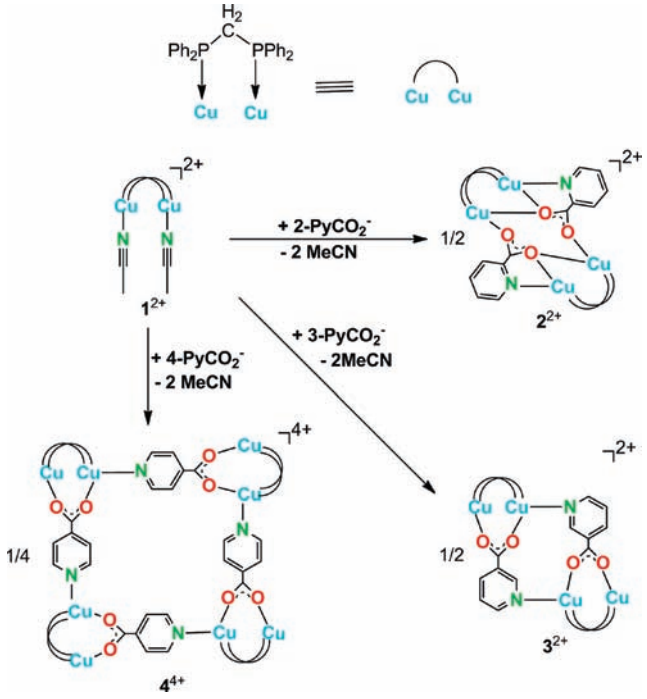

interactions with various oxyanions,[10] it is not surprising that the bonded nitrate anions of $[Cu_2(dppm)_2(NO_3)_2]$ impede the formation of polygonal oligomeric metallacycles; the reaction of the complex with 2-$PyCO_2H$ thus produces $[Cu_2(dppm)_2(\eta^2\text{-}(2\text{-}PyCO_2H)_2](NO_3)_2$.[11] In the present study, the cation with noncoordinating anions, $[Cu_2(dppm)_2(MeCN)_2]X_2$ (**1**X_2; $X^- = BF_4^-$, PF_6^-, or BPh_4^-), was found to readily self-assemble pyridylcarboxylates, 2-, 3-, and 4-$PyCO_2^-$, into distinctive polygonal oligomeric metallacycles, including dimeric, dimeric, and tetrameric structures, respectively (Scheme 1), as the only isolated, thermodynamically controlled, products in one-pot reactions. The results for the flexible ligand-coordinated cation $\mathbf{1}^{2+}$ hence contrast sharply with the mononuclear, trigonal, and square structures, obtained by Hor et al.,[6d] for the rigid ligand-capped cation, $[Pt(PPh_3)_2(MeCN)_2]^{2+}$. Importantly, the results indicate that a flexible ligand-capped dinuclear (and other multinuclear) transition-metal acceptor like $\mathbf{1}^{2+}$ can promote oligomerization for the 2-$PyCO_2^-$ donor and diminishes the shape difference between 2- and 3-$PyCO_2^-$ donors. The employment of a *flexible* ligand-capped transition-metal acceptor to replace a rigid analogue can bring unexpected structural variation in the products obtained by conventional directional bonding approach. However, the new oligomerization is still subject to steric or electronic hindrance, as demonstrated below.

Experimental Section

General Information. All reactions were performed under prepurified nitrogen using freshly distilled solvents. The IR spectra were recorded on a Bruker TENSOR 27 instrument. The ^{1}H and ^{31}P NMR spectra were recorded on a Bruker AVANCE 300 spectrometer (^{1}H, 300 MHz; ^{31}P, 122 MHz) or a Bruker AVANCE 500 spectrometer (^{1}H, 500 MHz; ^{31}P, 202 MHz) calibrated against internal deuterated solvents (^{1}H) or external 85% H_3PO_4 (^{31}P). Microanalyses were carried out by the staff of the Microanalytical Service of the Department of Chemistry, National Cheng Kung University. The dicopper(I) precursor complex, **1**X_2, was prepared according to a previously reported procedure.[7]

Synthesis of $[Cu_2(dppm)_2(2\text{-}PyCO_2)]_2(BF_4)_2$ (2$(BF_4)_2$). a. Method 1. Three drops of Et_3N (ca. 0.0333 mL, 0.0462 mmol) were added to a suspension of **1**$(BF_4)_2$ (0.1498 g, 0.130 mmol) and picolinic acid (0.0160 g, 0.130 mmol) in CH_2Cl_2 (25 mL), immediately forming a clear solution. The solution was stirred at ambient temperature for 10 min. All of the solvent and the excess Et_3N were removed by a vacuum pump to produce a pale yellow precipitate. The precipitate was washed with deaerated water (ca. 15 mL) and pumped dry. Recrystallization from CH_2Cl_2−hexane produced **2**$(BF_4)_2$. Yield 0.139 g, 97%. IR (CH_2Cl_2): $\nu_a(CO_2^-)$, 1603; $\nu_s(CO_2^-)$, 1404; $\nu(BF_4^-)$, 1098, 1060, 1038 cm^{-1}. ^{1}H NMR ($CDCl_3$, 296 K): δ 3.30 (s, 8 H, P-CH_2), 7.10−7.17 (m, 80 H, C_6H_5), 8.15 (m, 2 H), 8.56 (m, 2 H), 8.90 (m, 2 H), 9.03 (m, 2 H) for $PyCO_2^-$. ^{31}P{^{1}H} NMR ($CDCl_3$, 296 K): δ −7.66 (s). Elem anal. calcd for $C_{112}H_{96}B_2Cu_4F_8N_2O_4P_8$ (%): C, 60.88; H, 4.38; N, 1.27. Found: C, 60.54; H, 4.39; N, 1.26.

b. Method 2. A suspension of **1**$(BF_4)_2$ (0.1753 g, 0.152 mmol) and picolinic acid (0.0187 g, 0.152 mmol) in CH_2Cl_2 (25 mL) was stirred at ambient temperature for 30 min. The suspension formed a clear solution. The solution was then stirred for another 10 min. All of the solvent was removed by a vacuum pump to produce a pale yellow precipitate, which was then washed with Et_2O (ca. 25 mL) and collected. (If necessary, further recrystallization from CH_2Cl_2−hexane can be carried out.) Compound **2**$(BF_4)_2$ was produced. Yield: 0.163 g, 97%.

Synthesis of $[Cu_2(dppm)_2(3\text{-}PyCO_2)]_2(BF_4)_2$ (3$(BF_4)_2$). Compound **3**$(BF_4)_2$ was prepared in yields of 97% and 96% using procedures similar to those used in methods 1 and 2, respectively, for compound **2**$(BF_4)_2$. IR (CH_2Cl_2): $\nu_a(CO_2^-)$, 1603; $\nu_s(CO_2^-)$, 1402 cm^{-1}; $\nu(BF_4^-)$, 1098, 1060, 1038 cm^{-1}. ^{1}H NMR ($CDCl_3$, 296 K): δ 3.42 (s, 8 H, P-CH_2), 6.92−7.20 (m, 80 H, C_6H_5), 8.31 (m, 2 H), 8.91 (m, 2 H), 9.21 (m, 2 H), 9.47 (s, 2 H) for $PyCO_2^-$. ^{31}P{^{1}H} NMR ($CDCl_3$, 296 K): δ −8.01 (s). Elem anal. calcd for $C_{112}H_{96}B_2Cu_4F_8N_2O_4P_8$ (%): C, 60.88; H, 4.38; N, 1.27. Found: C, 61.13; H, 4.41; N, 1.25.

Synthesis of $[Cu_2(dppm)_2(4\text{-}PyCO_2)]_4(BF_4)_4$ (4$(BF_4)_4$). Compound **4**$(BF_4)_4$ was prepared in a yield of 97% using a procedure similar to that used in method 2 for compound **2**$(BF_4)_2$. IR (CH_2Cl_2): $\nu_a(CO_2^-)$, 1604; $\nu_s(CO_2^-)$, 1403 cm^{-1}; $\nu(BF_4^-)$, 1098, 1060, 1038 cm^{-1}. ^{1}H NMR (CD_2Cl_2, 296 K): δ 3.23 (s, 16 H, P-CH_2), 7.03−7.24 (m, 160 H, C_6H_5), 8.55 (d, 8 H, J = 5.7), 9.00 (d, 8 H, J = 5.7), for $PyCO_2^-$. ^{31}P{^{1}H} NMR ($CDCl_3$, 296 K): δ −7.94 (s). Elem anal. calcd for $C_{224}H_{192}B_4Cu_8F_{16}N_4O_8P_{16}$ (%): C, 60.88; H, 4.38; N, 1.27. Found: C, 61.01; H, 4.08; N, 1.19.

Synthesis of $[Cu_2(dppm)_2(6\text{-}Me\text{-}3\text{-}PyCO_2)](BF_4)$ (5(BF_4)). Compound **5**(BF_4) was prepared in a yield of 96% using a procedure similar to that used in method 2 for compound **2**$(BF_4)_2$. IR (CH_2Cl_2): $\nu_a(CO_2^-)$, 1600; $\nu_s(CO_2^-)$, 1404 cm^{-1}; $\nu(BF_4^-)$, 1103, 1061, 1038 cm^{-1}. ^{1}H NMR (CD_2Cl_2, 296 K): δ 2.87 (s, 3 H, CH_3), 3.17 (m, 4H, P-CH_2), 7.02−7.15 (m, 40 H, C_6H_5), 7.95 (d, 1 H, J = 4.4), 8.95 (d, 1 H, J = 4.4), 9.24 (s, 1 H) for $PyCO_2^-$. ^{31}P{^{1}H} NMR ($CDCl_3$, 296 K): δ −7.79 (s). Elem anal. calcd for $C_{57}H_{50}BCu_2F_4NO_2P_4$ (%): C, 61.19; H, 4.50; N, 1.25. Found: C, 61.15; H, 4.73; N, 1.25.

X-Ray Crystallography. Single crystals were obtained by layering hexane on top of a CH_2Cl_2 or CH_2Cl_2−MeOH solution of the complexes. Data collection was performed on a Bruker SMART-CCD diffractometer at 100(2) K for crystal **2**$(PF_6)_2$,

(8) The distance, d(Cu···Cu), of 3.426(3) Å found in the structure of $[Cu_2(dppm)_2(NCMe)_4](ClO_4)_2$[7] is much larger than the sum of the van der Waals radii of two Cu^I centers of 2.80 Å.[9]

(9) Bondi, A. *J. Phys. Chem.* **1964**, *68*, 441.
(10) Bera, J. K.; Nethaji, M.; Samuelson, A. G. *Inorg. Chem.* **1999**, *38*, 1725.
(11) Liu, Y.; Zhao, D.; Yang, R.; Zhu, J.; Sun, Y.; Zhang, C. *Russ. J. Inorg. Chem.* **2004**, *49*, 1828.

Table 1. Crystal Data

crystal	$2(PF_6)_2 \cdot 2CH_2Cl_2$	$3(PF_6)_2 \cdot 4CH_2Cl_2$	$4(BF_4)_4 \cdot CH_2Cl_2$	$5(BF_4) \cdot 4CH_2Cl_2$
formula	$C_{114}H_{100}Cl_4Cu_4F_{12}N_2O_4P_{10}$	$C_{116}H_{104}Cl_8Cu_4F_{12}N_2O_4P_{10}$	$C_{225}H_{194}B_2Cl_2Cu_8F_8N_4O_8P_{16}$	$C_{61}H_{59}B_2Cl_8Cu_2F_8NO_2P_4$
fw (g mol^{-1})	2495.62	2665.47	4330.20	1546.27
cryst size (mm^3)	0.20 × 0.15 × 0.15	0.15 × 0.10 × 0.10	1.00 × 0.80 × 0.20	1.00 × 0.80 × 0.60
cryst syst	monoclinic	monoclinic	triclinic	monoclinic
space group	$P2_1/c$	$P2_1/n$	$P\bar{1}$	$P2_1/c$
a (Å)	15.506(3)	12.0588(2)	14. 564(2)	12.578(5)
b (Å)	22.758(4)	25.3520(4)	22.880(3)	20.407(8)
c (Å)	16.992(3)	19.3009(3)	23.563(3)	27.288(10)
α (deg)	90	90	61.091(2)	90
β (deg)	113.779(3)	103.992(1)	80.927(2)	102.702(6)
γ (deg)	90	90	81.605(2)	90
V (Å^3)	5487.3(15)	5725.49(16)	6765.3(16)	6833(4)
Z	2	2	1	4
D_{calc} (g cm^{-3})	1.510	1.546	1.063	1.503
μ, (mm^{-1})	1.082	1.133	0.781	1.093
F(000)	2544	2712	2224	3136
reflns collected, unique	39430/13607	57689/10081	26542/26542	42559/14061
R_1/wR_2 ($I > 2\sigma(I)$)	0.0670/0.1581	0.0510/0.1218	0.0720/0.1754	0.0686/0.1901
GOF on F^2	0.867	1.077	0.817	1.039
largest diff peak and hole (e Å^{-3})	2.348/-1.507	0.586/-0.812	1.412/-0.480	1.320/-1.497

on a NONIUS Kappa CCD diffractometer at 150(2) K for crystal $3(PF_6)_2$, and on a Bruker SMART Apex II diffractometer at 296(2) K for a crystal of $4(BF_4)_4$ and at 100(2) K for crystal $5(BF_4)$. The three instruments were equipped with graphite-monochromated Mo Kα radiation (λ = 0.71073 Å). Empirical absorption corrections were made on the basis of an azimuthal scan. The structures of crystals were determined using the direct method and then refined using the full-matrix least-squares method on F^2, with all non-hydrogen atoms refined with anisotropic temperature parameters using SHELXL-97 software.[12] The PLATON-SQUEEZE program was applied to crystal $4(BF_4)_4$ for the position-disordered solvent molecules in the structure refinement.[13] Almost all hydrogen atoms were either located from the difference maps or generated by geometry with d(C−H) = 0.930 or 0.950 Å. A summary of the crystal data, data collection, and refinement parameters is provided in Table 1.

Results and Discussion

Synthesis, Solution Behavior, and Structures of Multicopper Metallacycles. As illustrated in Scheme 1, the synthesis of the multicopper metallacycles ($2X_2$−$4X_4$) was readily achieved by the direct treatment of the dicopper complex, $1X_2$, with 2-, 3-, and 4-$PyCO_2H$ in the presence or absence of Et_3N in CH_2Cl_2 at ambient temperature. The production yields for metallacycles $2X_2$, $3X_2$, and $4X_4$ were almost quantitative. However, the time-dependent $^{31}P\{^1H\}$ NMR spectra (Figure 1), obtained by mixing an equal amount of $[Cu_2(dppm)_2(MeCN)_2](BF_4)_2$ ($1(BF_4)_2$) and $PyCO_2H$ in CD_2Cl_2 in an NMR tube, indicate that metallacycles $2(BF_4)_2$ and $4(BF_4)_4$ formed almost completely, but that metallacycle $3(BF_4)_2$ and one unidentified product, $3u(BF_4)$, which resonate in $^{31}P\{^1H\}$ NMR experiments at δ −8.01 and −9.93, respectively, were in an equilibrium ratio of ca. 1:0.43, favoring metallacycle $3(BF_4)_2$, after 7 h. Following the removal of MeCN using a vacuum pump (see Experimental Section), metallacycle $3(BF_4)_2$ was obtained as the only product. The intensity of the signal at δ −8.01 increases upon the addition of pure metallacycle $3(BF_4)_2$,

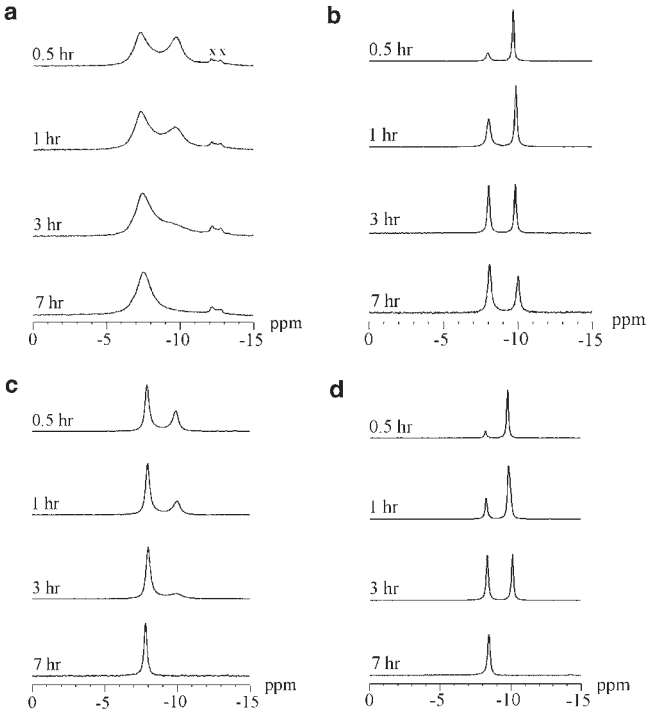

Figure 1. Time-dependent $^{31}P\{^1H\}$ NMR spectra for reactions (a) between complex $1X_2$ and 2-$PyCO_2H$ with signals for impurity marked by ×, (b) between complex $1X_2$ and 3-$PyCO_2H$, (c) between complex $1X_2$ and 4-$PyCO_2H$, and (d) between complex $1X_2$ and 6-Me-3-$PyCO_2H$ in CD_2Cl_2 at ambient temperature.

whereas the intensity of the signal at δ −9.93 increases immediately with a complete disappearance of the signal at δ −8.01 after the addition of one drop of MeCN (ca. 0.031 mL) into the NMR tube. Noteworthily, the ^1H NOESY spectra obtained[14] support that metallacycles $2(BF_4)_2$, $3(BF_4)_2$, and $4(BF_4)_4$ can react with the added MeCN molecules to form MeCN adducts. All the evidence

(12) Sheldrick, G. M. *SHELXTL-97*; University of Göttingen: Göttingen, Germany.

(13) Spek, A. L. *J. Appl. Crystallogr.* **2003**, *36*, 7.

(14) A typical NOESY experiment was performed using a solution of metallacycle (ca. 10^{-3}M) and MeCN (1 drop, ca. 0.03 mL) in CD_2Cl_2 (0.5 mL). In the NOESY spectrum, the methyl group of the added MeCN molecules shows a cross peak to the phenyl group of dppm in a metallacycle, 2^{2+}, 3^{2+}, or 4^{4+}.

Scheme 2

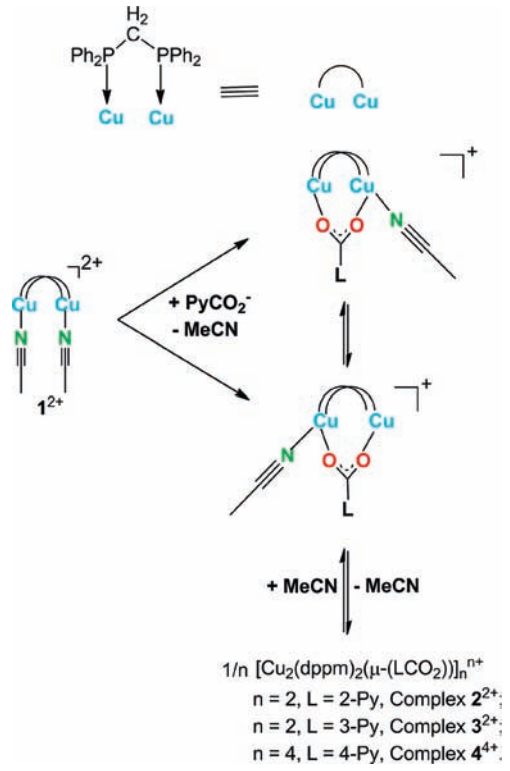

indicate that the adducts are probably $[Cu_2(dppm)_2(\mu\text{-}L)(MeCN)](BF_4)$ (L = 2-$PyCO_2$, **2u**(BF_4); 3-$PyCO_2$, **3u**(BF_4); and 4-$PyCO_2$, **4u**(BF_4)),[15] which are also in equilibrium with respective metallacycles (Scheme 2). Further, IR spectra of the CD_2Cl_2 solution used to measure the NOESY spectra contain two ν(CN) absorption bands,[17] one at 2291 cm^{-1} assigned to free MeCN molecules and the other at 2276, 2277, and 2272 cm^{-1} assigned to the coordinated MeCN molelcules in compounds **2u**(BF_4), **3u**(BF_4), and **4u**(BF_4), respectively. It is apparent that a metallacycle is a thermodynamically stable product from the reactions of complex $\mathbf{1}X_2$ with 2-, 3-, and 4-$PyCO_2H$ in CH_2Cl_2.

Three crystal structures, $[\{Cu_2(dppm)_2\}(\mu\text{-}(2\text{-}PyCO_2))]_2(PF_6)_2$ (**2**$(PF_6)_2$), $[\{Cu_2(dppm)_2\}(\mu\text{-}(3\text{-}PyCO_2))]_2(PF_6)_2$ (**3**$(PF_6)_2$), and $[\{Cu_2(dppm)_2\}(\mu\text{-}(4\text{-}PyCO_2))]_4(BF_4)_4$ (**4**$(BF_4)_4$), were determined using X-ray diffraction. ORTEP plots for cations $\mathbf{2}^{2+}$, $\mathbf{3}^{2+}$, and $\mathbf{4}^{4+}$ are presented in Figures 2, 3, and 4, respectively.

From the figures, it is evident that a dimerization occurs for 2-$PyCO_2^-$ and 3-$PyCO_2^-$, forming 8- and 12-membered metallacycles, respectively, whereas a tetramerization occurs for 4-$PyCO_2^-$, forming a 28-membered metallacycle. Two dimeric structures with diagonal distances of 4.711(10) Å (see Figure 2a) and of 7.035(5) Å (see Figure 3a) between Cu(1) and Cu(1′) are caused by two bonding modes adopted by pyridylcarboxylate donors, respectively. 2-$PyCO_2^-$ use one oxygen atom, O(1), and one nitrogen atom, N(1), to coordinate with a copper atom, Cu(2), forming a five-membered ring. O(1) also serves as a one-atom bridge, coordinating with Cu(1). This atom also links with the O(2′) of another 2-$PyCO_2^-$. Two carboxylate oxygen atoms, rather than the nitrogen atom, of one 2-$PyCO_2^-$ are hence involved in the skeleton of the eight-membered metallacycle (Figure 2a). However, 3-$PyCO_2^-$ uses two oxygen atoms, O(1) and O(2), to coordinate with copper atoms, Cu(1) and Cu(2), respectively. Cu(1) also links with N(1′) of another 3-$PyCO_2^-$. One of two carboxylate oxygen atoms and the nitrogen atom of one 3-$PyCO_2^-$ are thus involved in the skeleton of the 12-membered metallacycle (Figure 3a). The bonding

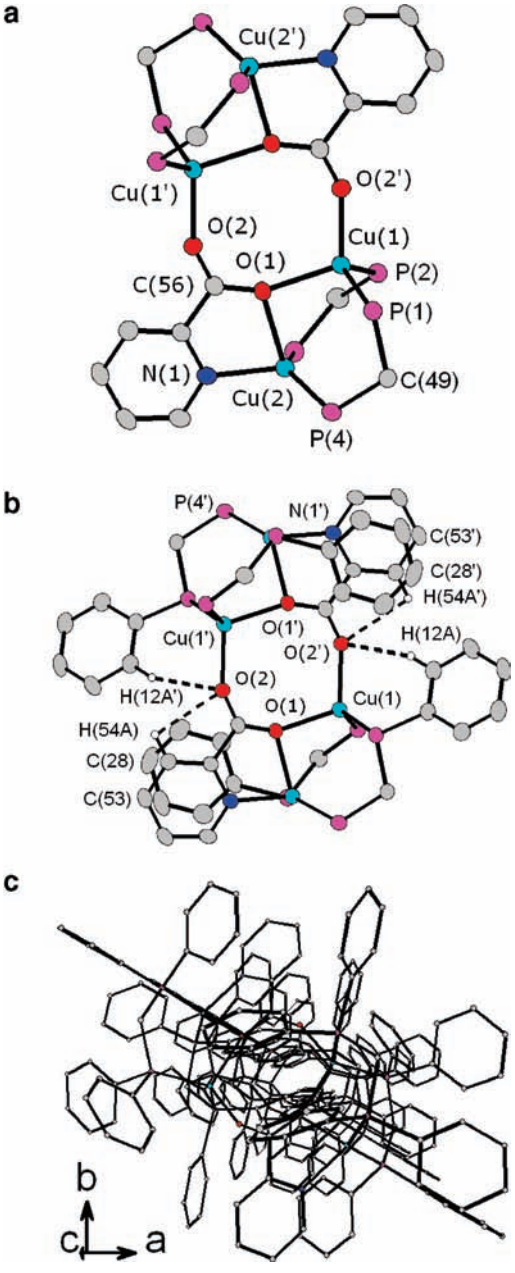

Figure 2. (a) Cation fragment of $[Cu_2(dppm)_2(2\text{-}PyCO_2)]_2(PF_6)_2$ (**2**$(PF_6)_2$) with phenyl rings on phosphorus and hydrogen atoms removed for clarity. (b) Secondary interactions with hydrogen bonds (shown as dashed lines) and $\pi-\pi$ stacking between two nearby phenyl planes, {N1, C50, C52, C53, C54, C55} and {C25, C26, C27, C28, C29, C30}. (c) 1D columnar packing of complex $\mathbf{2}^{2+}$, viewed along the *c* axis with hydrogen atoms omitted for clarity.

(15) The crystal structures of compounds $\mathbf{2u}^+$, $\mathbf{3u}^+$, and $\mathbf{4u}^+$ are believed to be similar to that observed for the cation of $[Cu_2(dppm)_2(\mu\text{-}OAc)(MeCN)](PF_6)$.[16]

(16) Shiu, K.-B.; Liu, S.-A.; Lee, G.-H. Unpublished Results.

(17) The detection of two ν(CN) absorption bands is reasonable given that the time scale for IR is much shorter than that for NMR spectroscopy.[18]

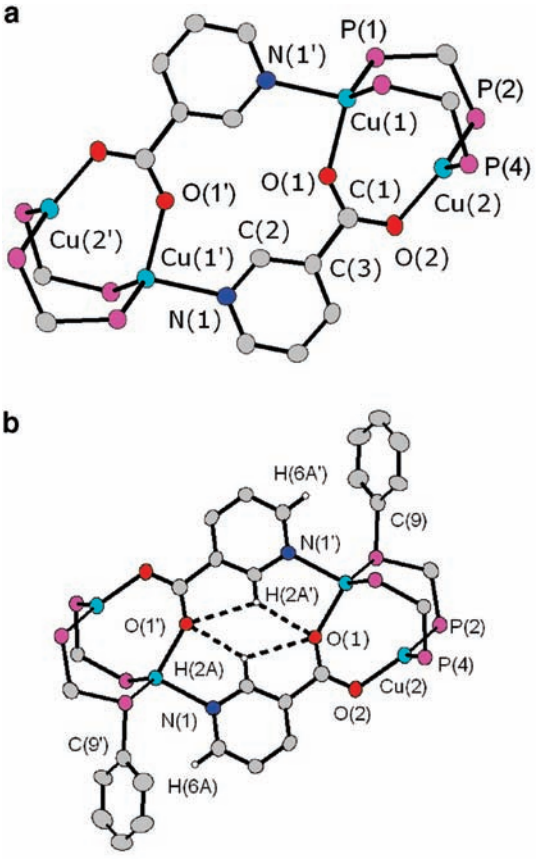

Figure 3. (a) Cation fragment of $[Cu_2(dppm)_2(3\text{-}PyCO_2)]_2(PF_6)_2$ (**3**$(PF_6)_2$) with phenyl rings on phosphorus and hydrogen atoms removed for clarity. (b) Secondary interactions with hydrogen bonds (shown as dashed lines) and C−H···π interaction between H(6A) and one nearby phenyl plane, {C9′, C10′, C11′, C12′, C13′, C14′}.

modes for 2- and 3-$PyCO_2^-$ were previously described in the structures of $[Cu_2(dppm)_2(\eta^2\text{-}(2\text{-}PyCO_2H)_2](NO_3)_2$[12] and $[Cu_2(dppm)_2(\mu\text{-}OAc)](BF_4)$.[19] Like the bonding mode of 3-$PyCO_2^-$, 4-$PyCO_2^-$ also uses two oxygen atoms, O(1) and O(2), to coordinate with copper atoms, Cu(1) and Cu(2), respectively. Cu(1) also links with the N(2) of another 4-$PyCO_2^-$. One of two carboxylate oxygen atoms and the nitrogen atom of one 4-$PyCO_2^-$ are involved in the skeleton of the 28-membered metallacycle with diagonal distances of 13.119(9) Å between Cu(1) and Cu(1′) and 12.641(11) Å between Cu(3) and Cu(3′) (Figure 4a). All of the copper atoms in structure $\mathbf{2}^{2+}$ are four-coordinate, whereas in structures $\mathbf{3}^{2+}$ and $\mathbf{4}^{4+}$, one-half of the copper atoms are three-coordinate and the other half are four-coordinate. The geometry adopted by a four-coordinate copper(I) atom is close to being tetrahedral, and that adopted by a three-coordinate copper(I) atom is close to being trigonal planar. Both geometries conform to simple structural models such as the VSEPR theory, because a Cu^I atom has a spherical (d^{10}) electron core.[20]

The flexible $\{Cu_2(dppm)_2\}$ unit of the starting complex, $[Cu_2(dppm)_2(NCMe)_2]X_2$ (**1**X_2), is believed to have a distance of around 3.4 Å between two copper atoms.[8]

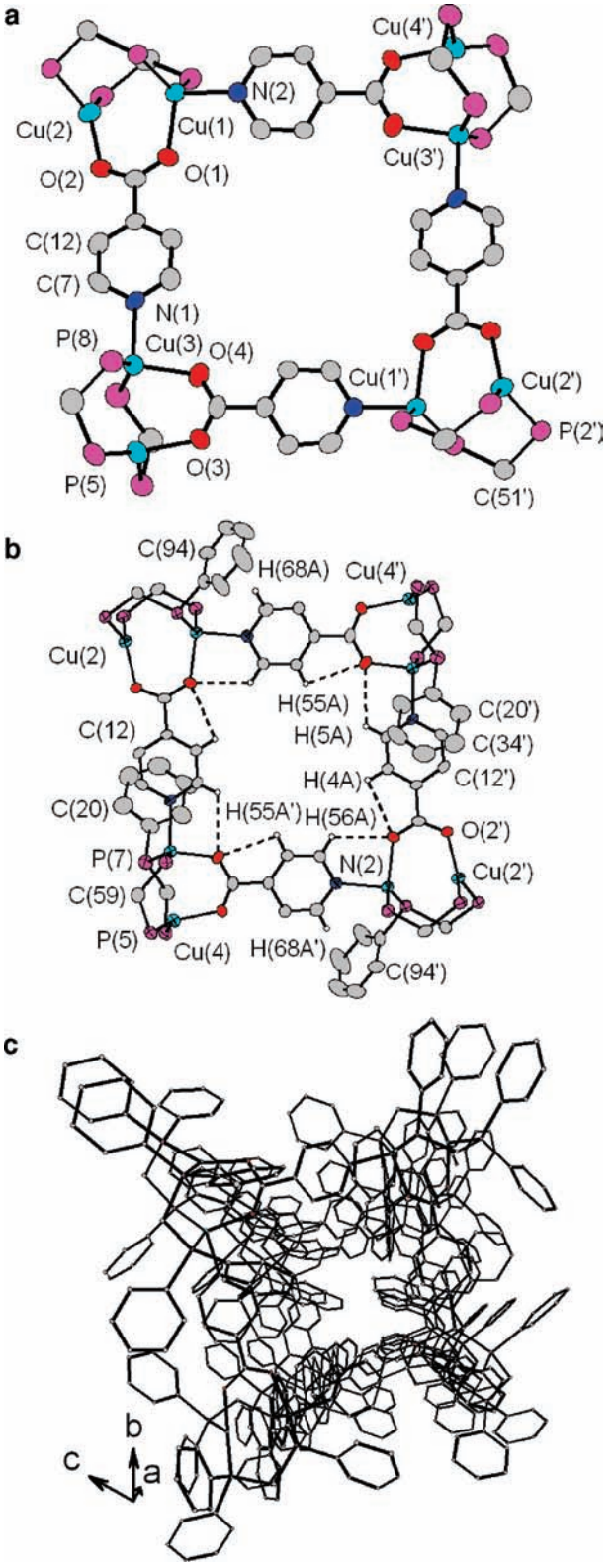

Figure 4. (a) Cation fragment of $[Cu_2(dppm)_2(4\text{-}PyCO_2)]_4(BF_4)_4$ (**4**$(BF_4)_4$) with phenyl rings on phosphorus and hydrogen atoms removed for clarity. (b) Secondary interactions with hydrogen bonds (shown as dashed lines) $\pi-\pi$ stacking between two nearby phenyl planes, {N1, C5, C4, C2, C12, C7} and {C13, C20, C34, C33, C40, C24}, and C−H···π interaction between H(68A) and one nearby phenyl plane, {C3, C22, C42, C27, C31, C94}. (c) 1D columnar packing for complex $\mathbf{4}^{4+}$, viewed along the *a* axis with hydrogen atoms omitted for clarity.

(18) Muetterties, E. L. *Inorg. Chem.* **1965**, *4*, 769.
(19) Harvey, P. D.; Drouin, M.; Zhang, T. *Inorg. Chem.* **1997**, *36*, 4998.
(20) (a) Kaupp, M. *Angew. Chem., Int. Ed.* **2001**, *40*, 3534. (b) Gillespie, R. J.; Robinson, E. A. *Chem. Soc. Rev.* **2005**, *34*, 396.

Table 2. Hydrogen Bonding Geometries (Å, deg) Existing in Cyclic Structures

structure	D−H···A	D−H	H···A	D···A	D−H···A
$\mathbf{2}^{2+}$	C12A−H12A···O2[a]	0.95	2.46	3.37	159.8
	C54A−H54A···O2	0.95	2.57	2.84	96.7
$\mathbf{3}^{2+}$	C2−H2A···O1	0.95	2.47	2.78	98.9
	C2−H2A···O1[b]	0.95	2.34	2.94	120.7
$\mathbf{4}^{4+}$	C4−H4A···O1	0.93	2.56	2.83	97.6
	C5−H5A···O4	0.93	2.67	3.20	116.6
	C55[c]−H55A[c]···O4	0.93	2.59	2.85	96.4
	C56−H56A···O1	0.93	2.50	3.09	121.8

[a] Symmetry transformation used to generate the equivalent atoms: $1-x, 1-y, 2-z$. [b] Symmetry transformation: $-x, -y, -z$. [c] Symmetry transformation: $1-x, 1-y, -z$.

Table 3. Phenyl−Phenyl Interactions Existing in Cyclic Structures

structure	interaction type	central separation (Å)	shortest contact (Å)	angle (deg)
$\mathbf{2}^{2+}$	$\pi-\pi$ stacking	3.85	3.78	$\beta = 10.94$
$\mathbf{3}^{2+}$	C−H···π	3.04[a]		$\theta = 157$
$\mathbf{4}^{4+}$	$\pi-\pi$ stacking	3.61	3.56	$\beta = 9.55$
	C−H···π	2.92[a]		$\theta = 151$

[a] Separation of an H atom and π ring centroid; θ = angle of C−H···ring centroid in C−H···π interaction; β = angle between the ring normal and centroid−centroid vector in $\pi-\pi$ stacking.

The nonbonded Cu···Cu distance shortens to 3.133(1) Å in cyclic structure $\mathbf{2}^{2+}$, 3.126(1) Å in structure $\mathbf{3}^{2+}$, and 2.968(2) Å and 2.833(4) Å in structure $\mathbf{4}^{4+}$. These values are within the reported range, 2.71−3.76 Å, for some typical complexes containing one or more $\{Cu_2(dppm)_2\}$-units.[19,21] However, among the four distances found in structures $\mathbf{2}^{2+}$, $\mathbf{3}^{2+}$, and $\mathbf{4}^{4+}$, it is surprising to have the longest Cu···Cu distance of 3.133(1) Å, rather than the shortest value, for the only structure, $\mathbf{2}^{2+}$, containing a one-atom bridge, O(1), linking the two Cu atoms of each $Cu_2(dppm)_2$ unit. A careful check of the structural details reveals the presence of secondary interactions, H-bonding (Table 2) and phenyl−phenyl interactions (Table 3), at different locations in the three structures. In structure $\mathbf{2}^{2+}$, four H-bonding interactions and two $\pi\cdots\pi$ (i.e., face-to-face) stacking interactions were found outside the dimeric metallacycle (Figure 2b). In structure $\mathbf{3}^{2+}$, four H-bonding interactions were found inside the dimeric metallacycle and two C−H···π (i.e., edge-to-face stacking) interactions were found outside the dimeric metallacycle (Figure 3b). In structure $\mathbf{4}^{4+}$, eight H-bonding interactions were found inside the tetrameric metallacycle, two $\pi\cdots\pi$ stacking interactions were found along the tetrameric metallacycle, and two C−H···π interactions were found outside the tetrameric metallacycle (Figure 4b). In the three structures, the H-bonding distances of 2.34−2.67 Å and angles of 96−160° (Table 2) are indicative of weak hydrogen bonding interactions.[22] The strength and location of the secondary interactions are believed to affect the Cu···Cu distances. Importantly,

(21) (a) Wu, M.-M.; Zhang, L.-Y.; Qin, Y.-H.; Chen, Z.-N. *Acta Crystallogr., Sect. E* **2003**, *59*, m195. (b) Jiang, K.; Zhao, D.; Guo, L.-B.; Zhang, C.-J.; Yang, R.-N. *Chin. J. Chem.* **2004**, *22*, 1297. (c) Guo, L.-B.; Zhao, D.; Zheng, X.; Zhang, X.; Yang, R. *Russ. J. Inorg. Chem.* **2005**, *50*, 1681. (d) Angaridis, P.; Cotton, F. A.; Petrukhina, M. A. *Inorg. Chim. Acta* **2001**, *324*, 318. (e) Chen, Y.-D.; Zhang, L.-Y.; Chen, Z.-N. *Chin. J. Struct. Chem.* **2004**, *23*, 395. (f) Yam, V. W.-W.; Lam, C.-H.; Cheung, K.-K. *Chem. Commun.* **2001**, 545.

(22) Steed, J. W.; Atwood, J. L. *Supramolecular Chemistry*; Wiley: New York, 2000; p 23.

Scheme 3

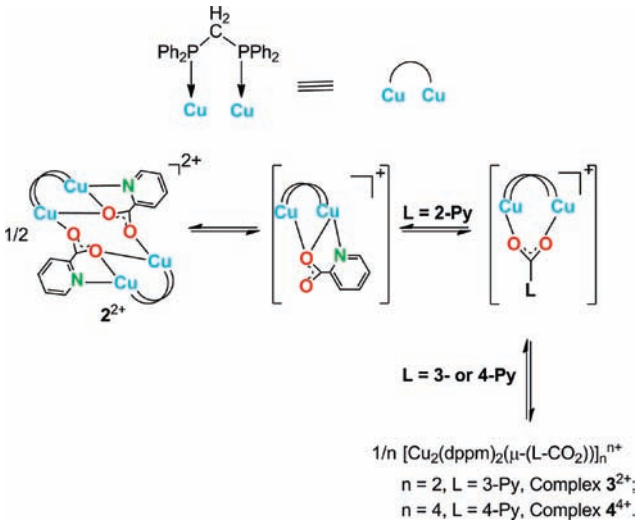

they may work cooperatively to help the observed cyclization in Scheme 1. The dimeric cycles for complex $\mathbf{2}^{2+}$ form 1D columns along the *a* axis (Figure 2c), but each column has a small rectangular cavity of 3.4 × 3.2 Å^2, where 3.4 Å is *d*(Cu(1)···C(56)) and 3.2 Å is *d*(Cu(1)···C(56′)) (Figure 2a). Although a similar cavity of 3.2 × 5.5 Å^2 is also found with 3.2 Å = *d*(Cu(1)···C(1)) and 5.5 Å = *d*(Cu(1)···C(1′)) (Figure 3a), the dimeric cycles for complex $\mathbf{3}^{2+}$ do not form 1D columns. This complex has nearly eclipsed dppm ligands with an average torsion angle of 8°, sterically impeding the 1D columnar packing. The dppm ligands for complex $\mathbf{2}^{2+}$ adopt a staggered conformation with an average torsion angle of 30°. Interestingly, for complex $\mathbf{4}^{4+}$, one-half of the dppm ligands adopt an eclipsed conformation with an average torsion angle of 10°, and the other half adopt a staggered conformation with an average torsion angle of 28°. The large cavity of 9.13 × 9.09 Å^2 with 9.13 Å = *d*(Cu(1)···Cu(3)) and 5.5 Å = *d*(Cu(1)···Cu(3′)) (Figure 4a) still allows the tetrameric cycles for complex $\mathbf{4}^{4+}$ to form 1D columns along the *c* axis (Figure 4c).

The solid-state structures indicate that cationic complexes $\mathbf{2}^{2+}$, $\mathbf{3}^{2+}$, and $\mathbf{4}^{4+}$ have point-group symmetries of C_{2h}, C_{2h}, and C_{4h}, respectively, in solution. Hence, the probable ^{31}P-spin systems assigned for the complexes are $A_2A'_2B_2B'_2$ for complex $\mathbf{2}^{2+}$, $A_2A'_2B_2B'_2$ for complex $\mathbf{3}^{2+}$, and $A_2A'_2A''_2A'''_2B_2B'_2B''_2B'''_2$ for complex $\mathbf{4}^{4+}$. However, unexpectedly, the $^{31}P\{^1H\}$ NMR spectra for the complexes (CD_2Cl_2, 202 MHz, 303 K) are very simple. Only one singlet was observed. When the measurement temperature was reduced to 203 K, only the signal for complex $\mathbf{3}^{2+}$ was broadened to have a shoulder in the upfield position. The signals for complexes $\mathbf{2}^{2+}$ and $\mathbf{4}^{4+}$ were simply broadened. When the number of scans was fixed at 100, the full width at half-maximum (FWHM) increased from 85.6 to 136.2 Hz and from 21.1 to 28.3 Hz for complex $\mathbf{2}^{2+}$ and complex $\mathbf{4}^{4+}$, respectively. With the crystal structures of $[Cu_2(dppm)_2(\mu\text{-OAc})](BF_4)$[19] and $[Cu_2(dppm)_2(6\text{-Me-3-PyCO}_2)](BF_4)$ (**5**(BF_4)), described below, it is proposed that a quick equilibrium between a probable intermediate, $[Cu_2(dppm)_2(LCO_2)]X$ (L = 2-, 3-, and 4-Py), and a metallacycle occurs in solution at ambient temperature, producing the observed singlet

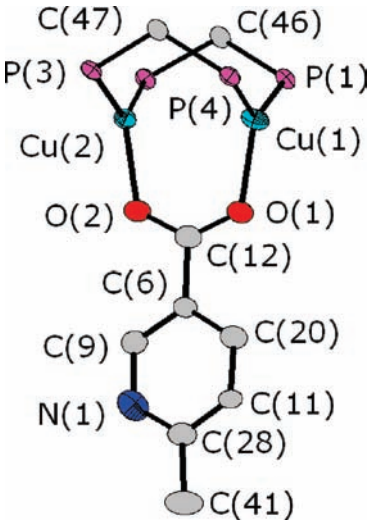

Figure 5. Cation fragment of $[Cu_2(dppm)_2(6\text{-Me-3-PyCO}_2)](BF_4)$ (**5**(BF_4)) with phenyl rings on phosphorus and hydrogen atoms removed for clarity.

signals for the complexes in the $^{31}P\{^1H\}$ NMR spectra (Scheme 3). With L = 2-Py, the intermediate may rearrange to form another intermediate, containing a (N,O)-linked geometry similar to that observed for $[Cu_2(dppm)_2(\eta^2\text{-}(2\text{-PyCO}_2H)_2](NO_3)_2$.[11] Thus, the cyclization probably starts with the replacement of MeCN of complex $\mathbf{1}X_2$ with LCO_2^- to form one or two intermediates depending on the identity of L, which then cyclize to form metallacycles $\mathbf{2}^{2+}$, $\mathbf{3}^{2+}$, and $\mathbf{4}^{4+}$.

Synthesis, Solution Behavior, and Structure of Uncyclized Dicopper Complex 5(BF_4). Since one of the favorable secondary interactions involves a hydrogen atom, H(6A), at a ring position next to the nitrogen atom, N(1), of 3-$PyCO_2^-$ in structure $\mathbf{3}^{2+}$ (Figure 3b), a simple replacement of the hydrogen atom with a methyl group may destroy the favorable interaction by introducing steric hindrance. Indeed, when 6-Me-3-$PyCO_2^-$ was used to react with$[Cu_2(dppm)_2(MeCN)_2](BF_4)_2$ (**1**), the expected oligomerization was inhibited, and the reaction produced a dinuclear product, $[Cu_2(dppm)_2(6\text{-Me-3-PyCO}_2)](BF_4)$ (**5**(BF_4)) (Figure 1d). The crystal structure of this complex was also determined by X-ray diffraction (Figure 5). The Cu−O distances of 2.029(4) and 2.015(4) Å are similar to those of 2.029(18) and 1.993(15) Å in $[Cu_2(dppm)_2(\mu\text{-OAC})](BF_4)$.[19] Likewise, the Cu···Cu distance of 2.869(5) Å in **5**(BF_4) is also similar to that of 2.789(11) Å in $[Cu_2(dppm)_2(\mu\text{-OAC})](BF_4)$.

Conclusion

The self-assemby of supramolecular metallacycles via the coordination-driven directional bonding approach can be modified to produce some unexpected structural variations via the employment of a flexible ligand-capped di- or multinuclear transition-metal acceptor like complex $\mathbf{1}X_2$ and a mixed-type donor like pyridylcarboxylate. However, the modified self-assembly is still subject to steric hindrance. The reaction of complex $\mathbf{1}(BF_4)_2$ with 6-Me-3-$PyCO_2H$ did not produce a polygonal dimeric metallacycle but a dinuclear complex, $[Cu_2(dppm)_2(6\text{-Me-3-PyCO}_2)](BF_4)$ (**5**(BF_4)).

Acknowledgment. This work was financially supported by the National Science Council of the Republic of China (under grant NSC95-2113-M-006-012-MY3).

Supporting Information Available: X-ray crystallographic data, in CIF format, and three ^1H NOESY spectra. This material is available free of charge via the Internet at http://pubs.acs.org.